Issues on the Geometry of Central Catadioptric Image Formation

João P. Barreto

Institute of Systems and Robotics
Dept. of Electrical and Computer Engineering
University of Coimbra
3030 Coimbra - PORTUGAL
jpbar@isr.uc.pt

Helder Araujo

Institute of Systems and Robotics
Dept. of Electrical and Computer Engineering
University of Coimbra
3030 Coimbra - PORTUGAL
helder@isr.uc.pt

Abstract

An imaging system with a single effective viewpoint is called a central projection system. The conventional perspective camera is an example of a central projection system. Systems using mirrors to enhance the field of view while keeping a unique center of projection are also examples of central projection systems. Perspective image formation can be described by a linear model with well known properties. In general central catadioptric imaging the mapping between points in the world and in the image is highly non-linear. This paper establishes a general model for central catadioptric image formation made up of three functions: a linear function mapping the world into an oriented projective plane, a non-linear transformation between two oriented projective planes, and a collineation in the plane. The model is used to study issues in the projection of lines. The equations and geometric properties of general catadioptric imaging of lines are derived. The application of the results in auto-calibration of central catadioptric systems and reconstruction are discussed. A method to calibrate the system using three line images is presented.

1. Introduction

Many applications in computer vision, such as surveillance and model acquisition for virtual reality, require that a large field of view is imaged. Visual control of motion can also benefit from enhanced fields of view. Computation of camera motion from a sequence of images obtained with a traditional camera suffers from the problem that the direction of translation may lie outside the field of view. Panoramic imaging overcomes this problem making the uncertainty of camera motion estimation independent of the motion direction [1, 2]. In image based visual servoing keeping the target in the field of view during motion raises severe difficulties. With a large field of view this problem no longer exists. One effective way to enhance the field of view of a camera is to use mirrors. The general approach of combining mirrors with conventional imaging systems is referred to as catadioptric image formation [3].

The fixed viewpoint constraint is a requirement ensuring that the visual sensor only measures the intensity of light passing through a single point in 3D space (the projection center). Vision systems verifying the fixed viewpoint constraint are called central projection systems. The well known perspective camera is an example of a central projection imaging system. Central projection systems present interesting geometric properties. A single effective viewpoint is a necessary condition for the generation of geometrically correct perspective images [4], and for the existence of epipolar geometry inherent to the moving sensor and independent of the scene structure [5]. It is highly desirable for any vision system to have a single viewpoint. In [4], Baker et al. derive the entire class of catadioptric systems with a single effective viewpoint. Systems built using a a parabolic mirror with an orthographic camera, or an hyperbolic, elliptical or planar mirror with a perspective camera verify the fixed viewpoint constraint.

A catadioptric realization of omnidirectional vision combines reflective surfaces and lenses. Catadioptric imaging systems that preserve the uniqueness of the projection viewpoint are called central catadioptric systems. Central catadioptric imaging can be highly advantageous for many applications because it combines two important features: a single projection center and a wide field of view. The drawback of this type of sensors is that in general the mapping between points in the 3D world and in the image is highly non-linear. This paper investigates the geometry of central catadioptric image formation. Perspective image formation can be described by a linear model with well known geometric properties. Many times correct perspective images are generated from frames captured by catadioptric sensors, and subsequently processed. We wish to study the advantages of working directly with the catadioptric images without warping them. Applications using information directly extracted from panoramic images can only be developed

Parabolic	$\sqrt{x^2+y^2+z^2} = 2p - z$
Hyperbolic	$\frac{(z-\frac{d}{2})^2}{a^2} - \frac{x^2}{b^2} - \frac{y^2}{b^2} = 1$
Elliptical	$\frac{(z-\frac{d}{2})^2}{a^2} + \frac{x^2}{b^2} + \frac{y^2}{b^2} = 1$
Planar	$z = \frac{d}{2}$

Table 1: Different mirror surfaces.

if the geometry of central catadioptric image formation is known.

In [6], Geyer and al. introduce an unifying theory for all central catadioptric systems. They show that central panoramic projection is isomorphic to a projective mapping from the sphere to a plane with a projection center on the perpendicular to the plane. The present paper starts by presenting a general framework to describe central catadioptric image formation. The mapping between point in 3D world and points in the catadioptric image is split into three steps. World points are mapped into an oriented projective plane by a linear function described by a 3×4 matrix (similar to the projective camera model referred to in [7]). The oriented projective plane is then transformed by a non-linear function $\mathbf{f}()$. The last step is a collineation in the plane depending on the mirror parameters, the pose of the camera in relation to the reflective surface and the camera intrinsic parameters. The model obtained is general, intuitive and isolates the non-linear characteristics of general catadioptric image formation.

A line in 3D projects into a conic in a general catadioptric image. The equations and geometric properties of the resulting conic are derived in [6]. In [6, 8] the intrinsic calibration of central catadioptric systems using line projections is discussed. A method to calibrate a system consisting of a paraboloid and an orthographic lens using two sets of parallel lines is presented in [8]. Our work uses the established mapping model to derive the equations and geometric properties of general central catadioptric line projection. Reconstruction aspects are discussed. It is shown that the plane collineation in the last step of our mapping model can be recovered from the images of three lines without further restrictions. This collineation depends on the system parameters and can be used to extract the calibration information.

2. Modelling Central Catadioptric Image Formation

This section establishes an unifying model for central projection panoramic imaging. The proposed model is valid for all catadioptric systems that verify the fixed viewpoint constraint as described in [2].

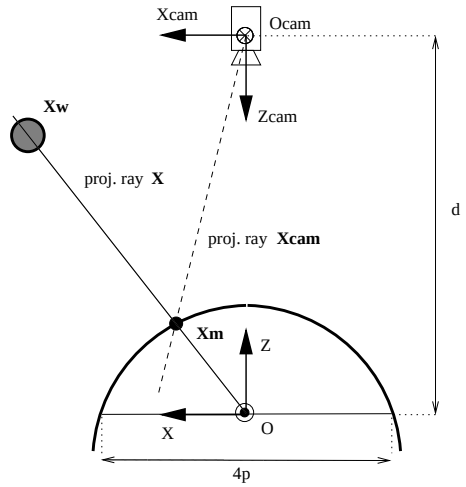

Figure 1: Central catadioptric vision system

2.1 Central Projection Catadioptric Systems

Fig.1 is a scheme of a central catadioptric vision system combining an hyperbolic reflective surface with a perspective camera. Assume an hyperbola is placed such that its axis is the z-axis, its foci are coincident with $\mathbf{O}$ and $\mathbf{O_{cam}}$ (the origin of coordinate systems $\Re$ and $\Re_{\mathbf{cam}}$), its latus rectum is $4p$ and the distance between the foci is d. The equation of the corresponding hyperbolic surface is given in Tab.1 with $a = \frac{1}{2}(\sqrt{d^2+4p^2} - 2p)$ and $b = \sqrt{p(\sqrt{d^2+4p^2} - 2p)}$. Consider a mirror with the shape of the lower branch of this central quadric. Light rays incident with $\mathbf{O}$ (the inner focal point) are reflected into rays incident with $\mathbf{O_{cam}}$ (the outer focal point). Assume a perspective camera with projection center in $\mathbf{O_{cam}}$ pointed to the mirror surface. All the captured light rays go originally through the inner focus of the hyperbolic surface. The effective viewpoint of the grabbed image is $\mathbf{O}$ and is unique.

Elliptical catadioptric images are obtained combining an elliptical mirror with a perspective camera in a similar way. For this case the light rays captured by perspective camera are reflected by the inner surface of a cut ellipsoid with foci in $\mathbf{O}$ and $\mathbf{O_{cam}}$ and latus rectum $4p$. The equation of the elliptical reflective surface is given in Tab.1 where $a = \frac{1}{2}(\sqrt{d^2+4p^2} + 2p)$ and $b = \sqrt{p(\sqrt{d^2+4p^2} + 2p)}$.

Assume now a parabolic reflective surface placed such that its axis is the z-axis, and its unique finite real focus is coincident with $\mathbf{O}$. Light rays incident with $\mathbf{O}$ are reflected into rays parallel with the z-axis. Consider an orthographic camera with image plane perpendicular to the z-axis. The camera only receives the light rays reflected by the mirror surface. The effective viewpoint is in $\mathbf{O}$ and is unique.

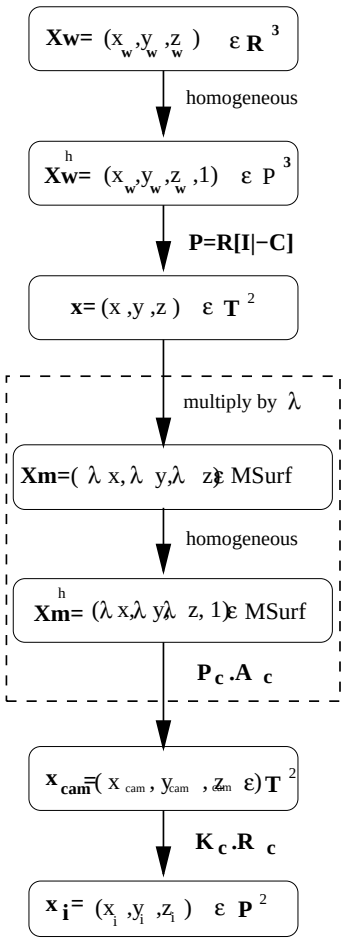

Figure 2: Mapping for different central catadioptric systems

A catadioptric system made up of a perspective camera steering a planar mirror also verifies the fixed view point constraint. The effective projection center is behind the mirror in the perpendicular line passing through camera center. Its distance to the camera center is twice the distance between the planar mirror and the camera. It will be shown that this is in many aspects a degenerate case of the central catadioptric projection. The geometry of planar catadioptric images is equivalent to conventional perspective imaging.

2.2 Mapping the World in a Catadioptric Image

Fig.2 illustrates the mapping performed by the different types of central catadioptric systems described in previous section. Consider a generic scene point, visible by the catadioptric system, with cartesian coordinates $\mathbf{X_w}$ in the world reference frame. The corresponding homogeneous representation is $\mathbf{X_w^h}$. Each visible point can be associated to a projective ray $\mathbf{x}$ joining the point with the effective viewpoint of the central projection system. $\mathbf{x} = \mathbf{P}\mathbf{X_w^h}$ where $\mathbf{P} = \mathbf{R}[\mathbf{I}| - \mathbf{C}]$ is a 3×4 matrix transforming points in the world reference frame in projective rays in the mirror coordinate system ($\mathbf{C}$ represents the world origin coordinates in the mirror reference frame, $\mathbf{R}$ is the rotation matrix between the coordinate systems and $\mathbf{I}$ is a 3×3 identity matrix). We can think of the projective rays $\mathbf{x}$ as points in an oriented projective plane $\mathbf{T^2}$. Notice that in standard projective geometry, given a projective point $\mathbf{x}$, $\lambda\mathbf{x}$ represents the same point whenever $\lambda \neq 0$. In an oriented projective plane this is only true if $\lambda > 0$ [11, 12]. This is important when modelling panoramic vision sensors where diametrically opposite points relative to the projection center can be simultaneously imaged.

	λ	$\mathbf{P_c}$	$\mathbf{R_c}$
Parabolic	$\frac{2p}{z+r}$	$\begin{bmatrix} 1 & 0 & 0 & 0 \\ 0 & 1 & 0 & 0 \\ 0 & 0 & 0 & 1 \end{bmatrix}$	$\mathbf{I}$
Hyperbolic	$\frac{2dp}{z(\sqrt{d^2+4p^2+2p})+dr}$	$[\mathbf{I}\|\mathbf{0}]$	any
Elliptical	$-\frac{2dp}{z(\sqrt{d^2+4p^2-2p})+dr}$	$[\mathbf{I}\|\mathbf{0}]$	any
Flat	$\frac{d}{2z}$	$[\mathbf{I}\|\mathbf{0}]$	any

Table 2: Mapping parameters (notice: $r = \sqrt{x^2 + y^2 + z^2}$)

To each projective ray $\mathbf{x}$ corresponds a projective ray $\mathbf{x_{cam}}$ going through the camera center. This one intersects the former in the mirror surface. The intersection point can be computed by scaling the projective ray $\mathbf{x}$ using a specific λ. $\mathbf{X_m} = \lambda\mathbf{x}$ are the coordinates of the point where the projective ray $\mathbf{x}$ intersects the mirror surface. The equations to compute λ are presented in Table.2. Notice that λ depends both on $\mathbf{x}$ and on the mirror surface. The corresponding projective ray in the camera coordinate system is $\mathbf{x_{cam}} = \mathbf{P_c}\mathbf{A_c}\mathbf{X_m^h}$. $\mathbf{A_c}$ is the 4×4 transformation matrix (rotation and translation) between mirror and camera coordinate systems and $\mathbf{A_c}\mathbf{X_m^h}$ is the intersection point in homogeneous camera coordinates. $\mathbf{P_c}$ is the 3×4 projection matrix that transforms this last point in the projective ray $\mathbf{x_{cam}}$. For the hyperbolic, elliptic and planar catadioptric system $\mathbf{P_c}$ is a perspective projection, for the parabolic catadioptric system $\mathbf{P_c}$ represents an orthographic projection (see Table.2).

In the case of the hyperbolic and elliptical systems, the fixed viewpoint constraint is verified whenever the camera center is coincident with the second focus of the reflective surface. There are no restrictions on the camera orientation. $\mathbf{R_c}$ is a 3×3 rotation matrix specifying the camera pose. The same can be said when using a planar mirror. For the parabolic situation the camera is orthographic with center

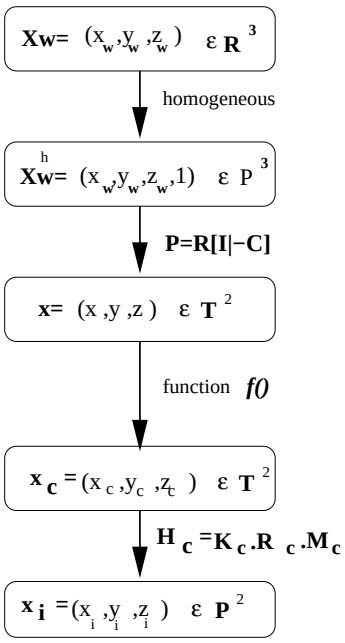

Figure 3: The new mapping model

at infinity. However there is an important restriction, its image plane must be orthogonal to the paraboloid axis. We are going to assume that $\mathbf{Rc} = \mathbf{I}$ for the parabolic mirror situation (see Table.2). $\mathbf{x_i} = \mathbf{K_c R_c x_{cam}}$ represents the point in the image plane where $\mathbf{K_c}$ is the matrix of camera intrinsic parameters.

2.3 The New Mapping Model

The mapping depicted in Fig.2 is general, covering all central catadioptric systems, in all possible configurations. Visible points in the scene $\mathbf{X_w^h}$ are mapped into projective rays/points $\mathbf{x}$ in the catadioptric system reference frame centered in the effective viewpoint. The transformation is linear being described by a 3×4 matrix $\mathbf{P}$. To each oriented projective ray/point $\mathbf{x}$, corresponds a projective ray/point $\mathbf{x_{cam}}$ in a coordinate system whose origin is in the camera projection center. Notice that $\mathbf{x}$ and $\mathbf{x_{cam}}$ must intersect in the mirror surface. We can think of this transformation as a non-linear mapping between two oriented projective planes. The relation between projective point $\mathbf{x_i}$ measured in the catadioptric image and $\mathbf{x_{cam}}$ is established by a collineation depending on camera orientation and intrinsic parameters.

$$\boldsymbol{x_{cam}} = \boldsymbol{M_c}.\boldsymbol{f}(\boldsymbol{x}) \tag{1}$$

$$\boldsymbol{M_c} = \begin{bmatrix} \psi - \xi & 0 & 0 \\ 0 & \xi - \psi & 0 \\ 0 & 0 & 1 \end{bmatrix} \tag{2}$$

	ξ	ψ
Parabolic	1	$1+2p$
Hyperbolic	$\frac{d}{\sqrt{d^2+4p^2}}$	$\frac{d+2p}{\sqrt{d^2+4p^2}}$
Elliptical	$\frac{d}{\sqrt{d^2+4p^2}}$	$\frac{d-2p}{\sqrt{d^2+4p^2}}$
Planar	0	1

Table 3: Mapping parameters ξ and ψ

$$\boldsymbol{f}(\boldsymbol{x}) = (\frac{x}{\sqrt{x^2+y^2+z^2}}, \frac{y}{\sqrt{x^2+y^2+z^2}}, \frac{z}{\sqrt{x^2+y^2+z^2}} + \xi)^t \tag{3}$$

For a conventional projective camera the mapping between points in the world and points in the image is linear if homogeneous coordinates are assumed [7]. In the model presented in last section all the transformations are linear with the exception of the mapping of $\mathbf{x}$ into $\mathbf{x_{cam}}$. As mentioned before we can think of $\mathbf{x}$ and $\mathbf{x_{cam}}$ as oriented projective points. The relationship between these two points is established by $\mathbf{x_{cam}} = \mathbf{F}(\mathbf{x})$ where $\mathbf{F}$ represents a non-linear correspondence between points in two different oriented projective planes. Thus $\lambda\mathbf{x_{cam}} = \lambda\mathbf{F}(\mathbf{x})$ whenever $\lambda > 0$. Using this property and after some algebraic manipulation the correspondence established by $\mathbf{F}()$ (the dotted area in Fig.2) can be written in the form of equation 1. The matrix $\mathbf{M_c}$ depends on the mirror parameters (see equation 2). The parameters ξ and ψ are presented in Table.3. Function $\mathbf{f}()$ is given by equation 3. Notice that $\mathbf{f}(\lambda\mathbf{x}) = \lambda\mathbf{x}$ whenever $\lambda > 0$. $\mathbf{f}()$ is a positive homogeneous function and correspondence $\mathbf{x_c} = \mathbf{f}(\mathbf{x})$ can be interpreted as a non-linear mapping between two oriented projective planes.

$$\boldsymbol{x_i} = \boldsymbol{H_c}.\boldsymbol{f}(\boldsymbol{P}.\boldsymbol{X_w^h}) \tag{4}$$

$$\boldsymbol{H_c} = \boldsymbol{K_c}.\boldsymbol{R_c}.\boldsymbol{M_c} \tag{5}$$

Figure3 depicts a scheme of the proposed model for general central projection. The mapping between points in the world $\mathbf{X_w}$ and projective points in image $\mathbf{x_i}$ is given by equation 4. Points $\mathbf{X_w^h}$ in projective 3D space are transformed in points $\mathbf{x}$ in the oriented projective plane with origin in the effective viewpoint of the catadioptric systems ($\mathbf{x} = \mathbf{P}.\mathbf{X_w^h}$). Points $\mathbf{x}$ are mapped in points $\mathbf{x_c}$ in a second oriented projective plane. The correspondence function $\mathbf{x_c} = \mathbf{f}(\mathbf{x})$ is non-linear. Projective points $\mathbf{x_i}$ in catadioptric image plane are obtained after a collineation $\mathbf{H_c}$ ($\mathbf{x_i} = \mathbf{H_c x_c}$).

Figure4 depicts an intuitive "concrete" model for the proposed general central projection mapping. To each vis-

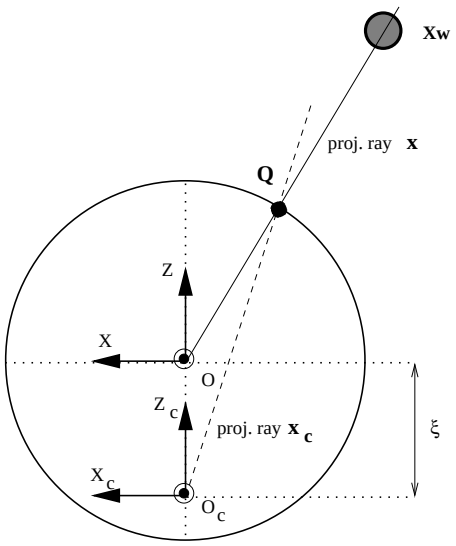

Figure 4: "Concrete" model for central catadioptric image formation

ible point in space corresponds an oriented projective ray $\mathbf{x}$ joining the 3D point with the effective projection center $\mathbf{O}$. The projective ray intersects a unit sphere centered in $\mathbf{O}$ in a unique point $\mathbf{Q}$. Consider a point $\mathbf{O_c}$ with coordinates $(0, 0, -\xi)^t$ in sphere reference frame $\Re$. To each $\mathbf{x}$ corresponds an oriented projective ray $\mathbf{x_c}$ joining $\mathbf{O_c}$ with the intersection point $\mathbf{Q}$ in the sphere surface. Points in catadioptric image plane x_i (not represented in the figure) are obtained after a collineation $\mathbf{H_c}$ of 2D projective points $\mathbf{x_c}$. The scene is projected in the sphere surface and then points on the sphere are re-projected in catadioptric image plane from a novel projection center $\mathbf{O_c}$. Point $\mathbf{O_c} = (0, 0, -\xi)^t$ only depends on mirror parameters (see Table.3). For a parabolic mirror $\xi = 1$ and $\mathbf{O_c}$ belongs to the sphere surface. The re-projection is a stereographic projection. For hyperbolic and elliptical case $\mathbf{O_c}$ is inside the sphere in the negative z-axis. The planar mirror is a degenerate case of central catadioptric projection where $\xi = 0$ and $\mathbf{O_c}$ is coincident with $\mathbf{O}$. The mapping of equation 4 is linear and the model becomes equivalent to the conventional model for projective cameras.

$$\boldsymbol{f^{-1}(x_c)} = (\lambda_c x_c, \lambda_c y_c, \lambda_c z_c - \xi)^t \tag{6}$$

$$\lambda_c = \frac{z_c\xi + \sqrt{z_c^2 + (1-\xi^2)(x_c^2 + y_c^2)}}{x_c^2 + y_c^2 + z_c^2} \tag{7}$$

To each projective ray $\mathbf{x}$ corresponds one, and only one, projective ray $\mathbf{x_c}$. Thus $\mathbf{f}()$ is homogeneous positive injective function with an inverse $\mathbf{f^{-1}}()$. The inverse function $\mathbf{f^{-1}}()$ maps points $\mathbf{x_c}$ in one oriented projective plane, in points $\mathbf{x}$ in another oriented projective plane ($\mathbf{x} = \mathbf{f^{-1}(x_c)}$). Once again $\mathbf{f^{-1}}()$ is a non-linear function (see equation 6).

3 Line Imaging in General Central Catadioptric Projection

This section focus on line imaging by a central catadioptric vision system. The model for central catadioptric image formation proposed in the previous section is used to derive the equations and geometric properties of line imaging.

Without loss of generality we are going to assume that world reference frame is aligned with catadioptric reference frame ($\mathbf{P} = [\mathbf{I}|\mathbf{0}]$). It is also assumed that $\mathbf{H_c} = \mathbf{I}$. By doing this the study will focus on the non-linear $\mathbf{f}()$ mapping. The image obtained only differs from the real catadioptric image by a familiar standard collineation between two projective planes.

A planar catadioptric system is a degenerate case of a central catadioptric projection. The mapping is similar to conventional projective cameras. Thus the study will focus only on parabolic, hyperbolic and elliptical projection ($\xi \neq 0$).

3.1 The Conic Image of a Line in the Scene

Assume a line in the scene contained by a plane $\mathbf{\Pi} = (l_x, l_y, l_z, 0)^t$ going through the origin $\mathbf{O}$ of the catadioptric system. The line projects in $\mathbf{l} = \mathbf{P^t}.\mathbf{\Pi}$. Since $\mathbf{P} = [\mathbf{I}|\mathbf{0}]$ then $\mathbf{l} = (l_x, l_y, l_z)^t$.

$$\boldsymbol{l^t.x} = 0 \Leftrightarrow l_x x + l_y y + l_z z = 0 \tag{8}$$

$$\boldsymbol{C} = \begin{bmatrix} l_x^2(1-\xi^2) - l_z^2\xi^2 & l_x l_y(1-\xi^2) & l_x l_z \\ l_x l_y(1-\xi^2) & l_y^2(1-\xi^2) - l_z^2\xi^2 & l_y l_z \\ l_x l_z & l_y l_z & l_z^2 \end{bmatrix} \tag{9}$$

Projective points $\mathbf{x}$ belonging to line $\mathbf{l}$ satisfy equation 8. In the previous section it was shown that $\mathbf{x} = \mathbf{f^{-1}}(\mathbf{x_c})$ (equation 6). The quadratic equation $\mathbf{x_c^t C x_c} = 0$ is obtained, after some algebraic manipulation, by replacing $\mathbf{x}$ by $\mathbf{x_c}$ in equation 8. The line is mapped into a conic $\mathbf{C}$ in the catadioptric image plane. The projective conic $\mathbf{C}$ is given in equation 9. Fig.5 shows this result considering the sphere model for central catadioptric projection. The line in space is projected into a great circle in the sphere surface. This great circle is the curve of intersection of plane $\mathbf{\Pi}$, containing the line and the projection center $\mathbf{O}$, and the unit sphere. The projective rays $\mathbf{x_c}$, joining $\mathbf{O_c}$ to points in the great circle, form a cone surface. The cone surface, with vertex in the $\mathbf{O_c}$, projects into the conic $\mathbf{C}$ in the canonical image plane. Notice that we can always think of a conic $\mathbf{C}$ in the projective plane as central cone of projective rays with vertex in the projection center.

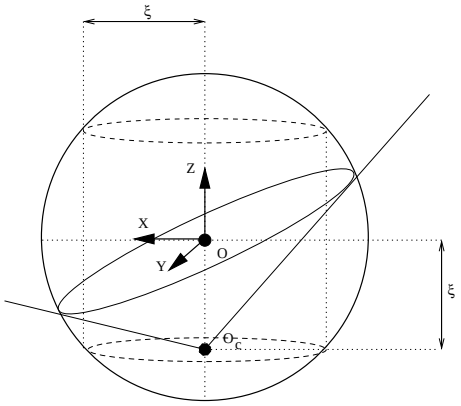

Figure 5: Model for line image formation in central catadioptric

Center	$(l_x l_z, l_y l_z, -\Delta)^t$
Principal Axis	$(\Delta l_x, \Delta l_y, (l_x^2 + l_y^2) l_z)^t \; ; \; (-l_y, l_x, 0)^t$
Major and Minor Axis	$\frac{(l_x^2+l_y^2+l_z^2) l_z^2 \xi^2}{\Delta^2} \; ; \; \frac{l_x^2+l_y^2+l_z^2}{\lvert\Delta\rvert}$
Real Focus	$(\frac{l_x}{l_z+\sqrt{l_x^2+l_y^2+l_z^2\sqrt{1-l^2}}}, \frac{l_y}{l_z+\sqrt{l_x^2+l_y^2+l_z^2\sqrt{1-l^2}}}, 1)^t;$ $(\frac{l_x}{l_z-\sqrt{l_x^2+l_y^2+l_z^2\sqrt{1-l^2}}}, \frac{l_y}{l_z-\sqrt{l_x^2+l_y^2+l_z^2\sqrt{1-l^2}}}, 1)^t$

Table 4: Parameters of the conic resulting from catadioptric projection of a line contained by the plane $\mathbf{\Pi} = (l_x, l_y, l_z, 0)^t$

3.2 Additional geometric issues

$\mathbf{C}$ is a degenerate conic whenever $l_z = 0$. If the line is in a plane Π containing the z-axis of the catadioptric reference frame, its projection is a line. This can be easily understood using the sphere model for the mapping. From now on it will be assumed that $l_z \neq 0$. If $\xi = 1$ the conic $\mathbf{C}$ is always a circle, which means that parabolic line image is always a circle. This is also a well known result.

$$\Delta = (l_x^2 + l_y^2)(1 - \xi^2) - l_z^2 \xi \tag{10}$$

Equation 10 gives the conic discriminant Δ. If $\Delta > 0$ then $\mathbf{C}$ is an hyperbola, if $\Delta = 0$ then $\mathbf{C}$ is a parabola, and if $\Delta < 0$ then $\mathbf{C}$ is an ellipse or a circle. Consider the cylinder with radius ξ and axis coincident with the z-axis of catadioptric reference frame depicted in Fig.5. The cylinder intersects the unit sphere into two opposite circles. Consider the intersection point of the sphere with the normal to the plane Π containing the line in space and the corresponding great circle. If the intersection point is between the circles the line image is an hyperbola. If the intersection point is above or below the circles the line image is an ellipse. Whenever the intersection points is in the circles the line image is a parabola.

Table.4 summarizes the geometric parameters of the conic image $\mathbf{C}$ of a line in space. Notice that one of the principal axes always goes through the principal point of the image plane. Foci equations are only valid for central conics (ellipse and hyperbola). If $\mathbf{C}$ is a parabola there is only one real finite focus $\mathbf{F} = (l_x, l_y, 2l_z)^t$.

4. Reconstruction and auto-calibration

In the derived general central projection model the scene is projected on the surface of an unit sphere centered in the effective viewpoint $\mathbf{O}$. The catadioptric image is captured by a conventional perspective camera, with viewpoint in $\mathbf{O_c}$, that projects on a plane the points on the sphere surface. Notice that the points of the world imaged by the camera lie all on the sphere surface. This is an important restriction with interesting features for calibration and reconstruction.

4.1 Three lines projected on a sphere

Consider three lines in the world. They are in planes $\mathbf{\Pi_1}$, $\mathbf{\Pi_2}$ and $\mathbf{\Pi_3}$ all going through point $\mathbf{O}$. These planes must satisfy two conditions:

- the planes can not contain the z-axis of the catadioptric reference frame (the degenerate case when a line projects onto a line);
- the rank of matrix $[\mathbf{\Pi_1 \Pi_2 \Pi_3}]$ must be 3 (the planes do not belong to a pencil of planes intersecting on a line);

Each plane intersects the unit sphere on a great circle (Fig.6). Each pair of great circles intersect in two antipodal points $\mathbf{F_{ij}}$ and $\mathbf{B_{ij}}$. The conditions above imply the existence of six intersection points. The line $\mathbf{F_{ij} B_{ij}}$, contains the origin $\mathbf{O}$, and is the common direction of planes $\mathbf{\Pi_i}$ and $\mathbf{\Pi_j}$.

4.2 Relations with the Plane at Infinity

Consider the plane at infinity $\Pi_\infty = (0, 0, 0, 1)^t$ defined in the camera reference frame $\Re_\mathbf{c}$ centered in $\mathbf{O_c}$. To each

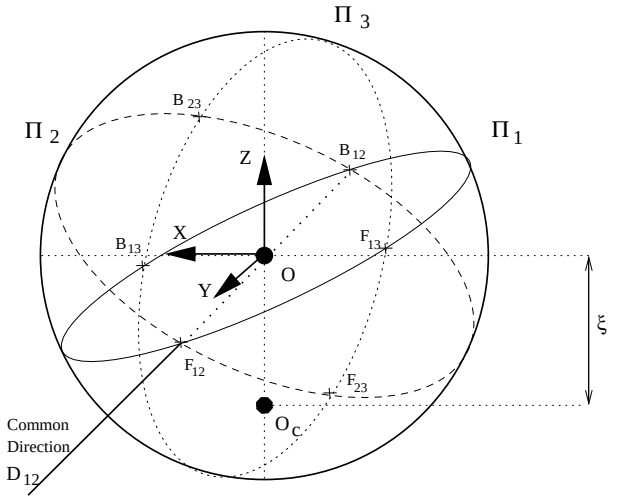

Figure 6: Three lines projected on the sphere surface. Each pair of great circles intersect in two antipodal points $\mathbf{F_{ij}}$ (front) and $\mathbf{B_{ij}}$ (back)

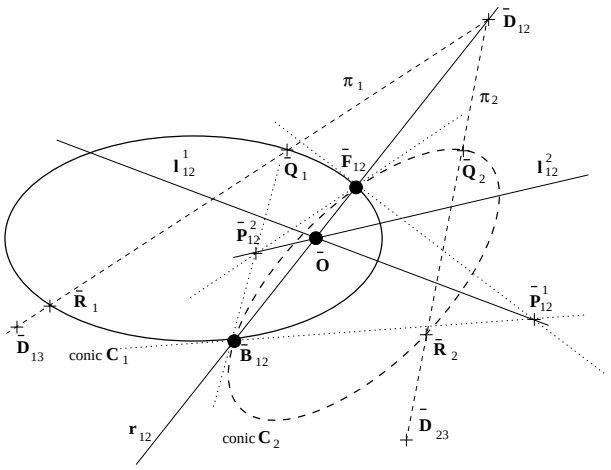

Figure 7: The plane at infinity

point $\mathbf{P}$ on the sphere, corresponds a projective ray going through the perspective camera center $\mathbf{O_c}$. The projective ray intersects the plane Π_∞ in the point $\bar{\mathbf{P}}$. Moreover a pencil of parallel planes intersects Π_∞ in the same line π (the horizon line) and a pencil of parallel lines intersects Π_∞ in the same point $\bar{\mathbf{D}}$ (the direction point). Each great circle depicted in Fig.6 defines a central cone of projective rays with vertex in $\mathbf{O_c}$. The intersection of a plane with a quadric is a conic curve, thus each central cone of projective rays intersects Π_∞ in a conic. Assume that $\mathbf{C_1}$, $\mathbf{C_2}$ and $\mathbf{C_3}$ are the conics associated to $\mathbf{\Pi_1}$, $\mathbf{\Pi_2}$ and $\mathbf{\Pi_3}$.

Fig.7 depicts $\mathbf{C_1}$ and $\mathbf{C_2}$ in $\mathbf{\Pi_\infty}$. The conics intersect in points $\bar{\mathbf{F}}_{\mathbf{12}}$ and $\bar{\mathbf{B}}_{\mathbf{12}}$. These two points define a line $\mathbf{r_{12}} = \bar{\mathbf{F}}_{\mathbf{12}} \wedge \bar{\mathbf{B}}_{\mathbf{12}}$. Similarly conics $\mathbf{C_2}$, $\mathbf{C_3}$ define $\mathbf{r_{23}}$ and $\mathbf{C_1}$, $\mathbf{C_3}$ define $\mathbf{r_{13}}$ (not depicted in Fig.7).

Proposition 1: *Consider* $\bar{\mathbf{O}}$ *the intersection point of the projective ray* $\mathbf{O_cO}$ *with* $\mathbf{\Pi_\infty}$. *Lines* $\mathbf{r_{12}}$, $\mathbf{r_{23}}$ *and* $\mathbf{r_{13}}$ *must intersect in* $\bar{\mathbf{O}}$.

Proof: The plane $\mathbf{O_cF_{12}B_{12}}$, which contains the origin $\mathbf{O}$ of the catadioptric system (see fig.6), intersects $\mathbf{\Pi_\infty}$ in the line $\mathbf{r_{12}}$. Thus the intersection of $\mathbf{O_cO}$ with $\mathbf{\Pi_\infty}$ must lie on $\mathbf{r_{12}}$. The same can be said about lines $\mathbf{r_{23}}$ and $\mathbf{r_{13}}$. Therefore $\mathbf{r_{12}}$, $\mathbf{r_{23}}$ and $\mathbf{r_{13}}$ must intersect in $\bar{\mathbf{O}}$.

Assume $\mathbf{C_1^*}$, $\mathbf{C_2^*}$ and $\mathbf{C_3^*}$ are the conic envelopes of $\mathbf{C_1}$, $\mathbf{C_2}$ and $\mathbf{C_3}$ [14], and that $\bar{\mathbf{D}}_{\mathbf{12}}$, $\bar{\mathbf{D}}_{\mathbf{23}}$ and $\bar{\mathbf{D}}_{\mathbf{13}}$ are the intersection points of space lines $\mathbf{F_{12}B_{12}}$, $\mathbf{F_{23}B_{23}}$ and $\mathbf{F_{13}B_{13}}$ with the plane at infinity. The following proposition refers to $\bar{\mathbf{D}}_{\mathbf{12}}$ but is extensible to $\bar{\mathbf{D}}_{\mathbf{23}}$ and $\bar{\mathbf{D}}_{\mathbf{13}}$.

Points $\bar{\mathbf{P}}^{\mathbf{1}}_{\mathbf{12}}$ and $\bar{\mathbf{P}}^{\mathbf{2}}_{\mathbf{12}}$ are the poles of line $\mathbf{r_{12}}$ with respect to conics $\mathbf{C_1}$ and $\mathbf{C_2}$ ($\bar{\mathbf{P}}^{\mathbf{1}}_{\mathbf{12}} = \mathbf{C_1^*r_{12}}$ and $\bar{\mathbf{P}}^{\mathbf{2}}_{\mathbf{12}} = \mathbf{C_2^*r_{12}}$).

Proposition 2: *Line* $\mathbf{F_{12}B_{12}}$ *is the common direction of planes* $\mathbf{\Pi_1}$ *and* $\mathbf{\Pi_2}$ *intersecting* $\mathbf{\Pi_\infty}$ *at* $\bar{\mathbf{D}}_{\mathbf{12}}$. *Assume that* $\mathbf{l^1_{12}}$ *is the line going through points* $\bar{\mathbf{O}}$ *and* $\bar{\mathbf{P}}^{\mathbf{1}}_{\mathbf{12}}$. *Point* $\bar{\mathbf{D}}_{\mathbf{12}}$ *is the pole of* $\mathbf{l^1_{12}}$ *with respect to conic* $\mathbf{C_1}$. *Moreover, if* $\mathbf{l^2_{12}}$ *is the line going through points* $\bar{\mathbf{O}}$ *and* $\bar{\mathbf{P}}^{\mathbf{2}}_{\mathbf{12}}$, *then* $\bar{\mathbf{D}}_{\mathbf{12}}$ *is also the pole of* $\mathbf{l^2_{12}}$ *with respect to conic* $\mathbf{C_2}$.

Proof: The line in space $\mathbf{F_{12}B_{12}}$ lies in plane $\mathbf{O_cF_{12}B_{12}}$. Thus point $\mathbf{D_{12}}$ must lie in line $\mathbf{r_{12}}$ at $\mathbf{\Pi_\infty}$. The pole of $\mathbf{r_{12}}$ with respect to conic $\mathbf{C_1}$ is $\bar{\mathbf{P}}^{\mathbf{1}}_{\mathbf{12}}$. Thus points $\bar{\mathbf{D}}_{\mathbf{12}}$ and $\bar{\mathbf{P}}^{\mathbf{1}}_{\mathbf{12}}$ are conjugate with respect to $\mathbf{C_1}$. The origin of the catadioptric system $\mathbf{O}$ lies in the line $\mathbf{F_{12}B_{12}}$ and is equidistant to points $\mathbf{F_{12}}$ and $\mathbf{B_{12}}$ (see Fig.6). This implies that, in the plane at infinity, points $\bar{\mathbf{D}}_{\mathbf{12}}$ and $\bar{\mathbf{O}}$ are harmonic with respect to $\bar{\mathbf{F}}_{\mathbf{12}}$ and $\bar{\mathbf{B}}_{\mathbf{12}}$. Thus $\bar{\mathbf{D}}_{\mathbf{12}}$ and $\bar{\mathbf{O}}$ are conjugate and $\mathbf{l^1_{12}} = \bar{\mathbf{P}}^{\mathbf{1}}_{\mathbf{12}} \wedge \bar{\mathbf{O}}$ is the polar line of $\bar{\mathbf{D}}_{\mathbf{12}}$ with respect to $\mathbf{C_1}$. Point $\bar{\mathbf{D}}_{\mathbf{12}}$ can be determined by making $\bar{\mathbf{D}}_{\mathbf{12}} = \mathbf{C_1^*l^1_{12}}$. The construction can also be made with respect to $\mathbf{C_2}$ yielding the same result.

Conics $\mathbf{C_2}$, $\mathbf{C_3}$ and $\mathbf{C_1}$, $\mathbf{C_3}$ can be used to determine $\mathbf{D_{23}}$ and $\mathbf{D_{13}}$ in a similar manner. Plane $\mathbf{\Pi_1}$ contains both directions $\mathbf{D_{12}}$ and $\mathbf{D_{13}}$. If π_1 is the intersection line of the plane with $\mathbf{\Pi_\infty}$ then π_1 must go through both $\mathbf{D_{12}}$ and $\mathbf{D_{13}}$ and $\pi_1 = \mathbf{D_{12}} \wedge \mathbf{D_{13}}$. Similarly $\pi_2 = \mathbf{D_{12}} \wedge \mathbf{D_{23}}$ and $\pi_3 = \mathbf{D_{23}} \wedge \mathbf{D_{13}}$. Notice that the rank of matrix $[\mathbf{\Pi_1\Pi_2\Pi_3}]$ must be 3, thus $\mathbf{D_{12}}$, $\mathbf{D_{23}}$ and $\mathbf{D_{13}}$ are never coincident.

Proposition 3: *In general a line intersects a conic in two points. Assume that* π_1 *and* $\mathbf{C_1}$ *intersect in* $\bar{\mathbf{Q}}_{\mathbf{1}}$ *and*

$\bar{\mathbf{R}}_1$, π_2 *and* $\mathbf{C}_2$ *intersect in* $\bar{\mathbf{Q}}_2$ *and* $\bar{\mathbf{R}}_2$, *and* π_3 *and* $\mathbf{C}_3$ *intersect in* $\bar{\mathbf{Q}}_3$ *and* $\bar{\mathbf{R}}_3$. *These six intersection points all belong to* $\boldsymbol{\Omega}_\infty$ *(the absolute conic in the plane at infinity [13]).*

Proof: In general a quadric in space intersects $\boldsymbol{\Pi}_\infty$ in a conic $\mathbf{C}$ which intersects $\boldsymbol{\Omega}_\infty$ in four points. Each pair of points defines a line to which corresponds a pencil of parallel planes (real or complex). This pencil of planes intersect the quadric in circular sections [9]. Conic $\mathbf{C_1}$ is the intersection of a central cone of projective rays $\mathbf{x_c}$ with the plane at infinity. Plane $\boldsymbol{\Pi}_1$ cuts this central cone in a circular section (see Fig.6) and the same applies to any plane parallel to $\boldsymbol{\Pi}_1$. Thus, the horizon line π_1 of the pencil of planes must go through two intersections points of $\mathbf{C_1}$ with $\boldsymbol{\Omega}_\infty$. This proves that the intersection points of π_1 and $\mathbf{C_1}$ lie in $\boldsymbol{\Omega}_\infty$. The same applies to points $\bar{\mathbf{Q}}_2$ and $\bar{\mathbf{R}}_2$, and $\bar{\mathbf{Q}}_3$ and $\bar{\mathbf{R}}_3$.

4.3 Applications to Auto-Calibration of Central Catadioptric Systems

Notice that the relationships established in the last section are projective invariants. They were derived using incidence and cross-ratios (pole/polar relationships with respect to conics).

As already mentioned the catadioptric image is captured by a conventional perspective camera, with viewpoint in $\mathbf{O_c}$, that projects in a plane the points on the sphere surface. It was assumed that collineation $\mathbf{H_c} = \mathbf{I}$ (see 3). The plane at infinity was defined in the camera reference frame with origin at camera center. Thus the three great circles represented in Fig.6 are imaged in $\mathbf{C_1}$, $\mathbf{C_2}$ and $\mathbf{C_3}$. The image plane cuts the central cones of projective rays $\mathbf{x_c}$ in the same conic lines as the plane at infinity. Moreover all the construction performed in previous section can be done in the image plane. Points $\bar{\mathbf{Q}}_1$, $\bar{\mathbf{R}}_1$, $\bar{\mathbf{Q}}_2$, $\bar{\mathbf{R}}_2$, $\bar{\mathbf{Q}}_3$ and $\bar{\mathbf{R}}_3$ belong, not to the absolute conic $\boldsymbol{\Omega}_\infty$, but to the image of the absolute conic $\boldsymbol{\Omega}$ (also equal to $\mathbf{I}$).

Consider that $\mathbf{H_c} \neq \mathbf{I}$ (which is the case in general). In this case the image of the absolute conic is $\boldsymbol{\Omega} = \mathbf{H_c^{-t}} \mathbf{H_c^{-1}}$. It depends on the camera intrinsic parameters, the camera pose and the mirror parameters. The procedure of previous section can be applied to estimate $\boldsymbol{\Omega}$ from the image of three lines in space. These lines are mapped into three conics in the image plane. The three conics intersect in six real points (which is assured by the restrictions that the planes containing the line satisfy). These intersection points are used to determine six points of $\boldsymbol{\Omega}$, as described. Since five points define a conic the six points are sufficient for the estimation of $\boldsymbol{\Omega}$.

5 Conclusions

In this paper we define a model for the image formation in central catadioptric systems. This general model is made up of three functions: a linear function mapping world points into an oriented projective plane, a non-linear transformation between between two oriented projective planes, and a collineation. This model enables the definition of a relationship between the images of lines and the parameters of the absolute conic. These relationships are used to develop a calibration method to estimate the parameters of the absolute conic.

References

[1] T. Svoboda, T. Pajdla and V. Hlavac, "Motion Estimation Using Central Panoramic Cameras," *Proc. IEEE Conference on Intelligent Vehicles, Stugart Germany 1998.*

[2] J. Gluckman and S. Nayar, " Egomotion and Omnidirectional Cameras," *ICCV98 - Proc. IEEE International Conference on Computer Vision*, pp. 999-1005, Bombay 1998.

[3] E. Hecht and A. Zajac, *Optics*, Addison-Wesley, 1974

[4] S. Baker and S. Nayar, "A Theory of Catadioptric Image Formation," *ICCV98 - Proc. IEEE International Conference on Computer Vision*, pp. 35-42, Bombay 1998.

[5] T. Svoboda, T. Pajdla and V. Hlavac, "Epipolar Geometry for Panoramic Cameras," *ECCV98- Proc. Of 5th European Conference on Computer Vision, pp 218-332, Freiburg Germany 1998.*

[6] C. Geyer and K. Daniilidis, "A Unifying Theory for Central Panoramic Systems and Pratical Implications," *ECCV2000- Proc. European Conference on Computer Vision*, pp. 445-461, Dublin 2000.

[7] R. Hartley and A. Zisserman, '*Multiple View geometry in Computer Vision*, Cambridge University Press, 2000.

[8] C. Geyer and K. Daniilidis, "Catadioptric Camera Calibration", *ICCV99 - Proc. of IEEE International Conference on Computer Vision*, pp. 398-403, Corfu, Greece, 1999.

[9] Barry Spain, *Analytical Quadrics*, Pergamon Press, 1960.

[10] Barry Spain, *Analytical Conics*, Pergamon Press, 1957.

[11] S. Laveau and O. Faugeras, "Oriented Projective Geometry for Computer Vision", *ECCV96 - Proc. of European Conference on Computer Vision*, 1996

[12] Jorge Stolfi, *Oriented Projective Geometry*, Academic Press Inc., 1991.

[13] O. Faugeras, *Three-dimensional computer vision, a Geometric Viewpoint*, MIT Press, 1993.

[14] J. G. Semple, G. T. Kneebone, *Algebraic Projective Geometry*, Clarendon Press, 1998.